International Scholarly Research Network
ISRN Pharmacology
Volume 2012, Article ID 417515, 8 pages
doi:10.5402/2012/417515

Research Article

Pharmacokinetics and Biodistribution Study of 7A7 Anti-Mouse Epidermal Growth Factor Receptor Monoclonal Antibody and Its $F(ab')_2$ Fragment in an Immunocompetent Mouse Model

Ailem Rabasa Capote,[1] Jorge Ernesto González,[2] Leyanis Rodríguez-Vera,[3] Armando López,[1] Belinda Sánchez Ramírez,[1] and Greta Garrido Hidalgo[1]

[1] *Tumor Immunology Direction, Molecular Immunology Institute, Center of Molecular Immunology, 216 Street, 15th Avenue, Atabey, Siboney, Playa, P.O. Box 16040, 11600 Havana, Cuba*
[2] *Departments of Pharmacology and Toxicology, Institute of Pharmacy and Foods, University of Havana, 11600 Havana, Cuba*
[3] *Radiobiology Laboratory, Center for Radiation Protection and Hygiene, 11600 Havana, Cuba*

Correspondence should be addressed to Ailem Rabasa Capote, ailem@cim.sld.cu

Received 8 October 2012; Accepted 23 October 2012

Academic Editors: K. Cimanga, G. Gervasini, T. Kumai, and T. B. Vree

Immunocompetent mice, Fc receptor γ-chain deficient mice ($Fcer1g^{-/-}$), and molecular tools as $F(ab')_2$ bivalent fragments appear as the most suitable biological models to study the mechanisms of the action of anti-epidermal growth factor receptor (EGFR) monoclonal antibodies (mAbs). *In vivo* experiments contrasting antitumor effects of whole Abs and their bivalent fragments commonly involve a previous comparative pharmacokinetics study. In this paper, pharmacokinetics and biodistribution of an anti-mouse EGFR Ab were assessed using immunocompetent mice. ^{125}I-labeled 7A7 mAb holds an elimination half-life ($t_{1/2}\beta$) of 23.1 h in C57BL/6 mice. Accumulation of mAb was found in liver, spleen, kidneys, and mostly in lungs. We used an ELISA method to determine the $t_{1/2}\beta$ of a 7A7 mAb using the same experimental setting. Results from this new analysis revealed a $t_{1/2}\beta$ of 23.9 h, supporting this method as a safer and easier system to evaluate pharmacokinetics parameters of mAbs targeting mouse EGFR. Using this system we also studied pharmacokinetics of 7A7 $F(ab')_2$ fragment. A tenfold difference between the mAb and fragment $t_{1/2}\beta$ was found. These data support the use of the 7A7 $F(ab')_2$ fragment in *in vivo* studies to explore the contribution of the EGFR signaling blockade and the Fc region to the antitumor effect of 7A7 mAb in this autologous scenario.

1. Introduction

Compelling experimental and clinical evidences support the relevance of EGFR as an attractive target for cancer therapy. EGFR-targeted immunotherapy based in mAb is clinically effective for advanced tumors of several localizations. Several anti-EGFR mAbs are being evaluated in various stages of clinical development, alone or in combination with radiotherapy and/or chemotherapy. Among these, cetuximab (Erbitux), panitumumab (Vectibix), and nimotuzumab (CIMAher) are the three EGFR-specific marketed mAbs [1]. Nimotuzumab was developed at the Center of Molecular Immunology (CIM) and is approved for the treatment of patients with head and neck [2, 3], high grade glioma [4], brainstem tumors [5], and esophagus tumors [6]. At the same time several clinical trials for other tumor indications are ongoing with promising results [7–9]. Despite encouraging results obtained in these trials, clinical benefit of anti-EGFR mAbs has been quite limited [10]. Special interest is being placed on the mechanisms underlying their antitumor activity which are not completely elucidated so far and might have a key role in patients' clinical responses. Investigations regarding anti-EGFR mAbs' effector mechanisms have been focused on the capacity of these agents to interfere with

EGFR signaling and the subsequent blockade of relevant pro-tumoral processes [11] and to induce Fc-mediated innate immune activation [12]. Recent preclinical and clinical data suggest the relevance of antibody-dependent cellular cytotoxicity (ADCC) as an immunological mechanism for cetuximab and panitumumab anti-tumor effect [13–16]. Nevertheless, the potential role that adaptive immunological mechanisms could play in the clinical response to anti-EGFR mAb-based immunotherapy is still under a wide focus of research. Clinical observations from trials with nimotuzumab or cetuximab evidence a delayed separation of the survival curves, indicating a non-proportional hazard ratio between treated and control patients along the follow-up time [3, 17]. These results suggest that short term mechanisms such as signaling inhibition and ADCC are not the only ones involved. A possible explanation would be a time-delayed induction of a protective T-cell-mediated immunity which could be associated with the clinical effect achieved. However, there is a lack of molecular and cellular evidences demonstrating the induction of T-cell activation by EGFR-specific mAbs and the contribution of this response to the antitumor effect in patients. In this regard, investigations in preclinical settings have suggested the contribution of anti-EGFR mAbs to immune response activation through its link with some elements of the adaptive immunity [18, 19]. At CIM, aiming to use immunocompetent mice in a complete autologous scenario, we generated 7A7 mAb specific for murine EGFR, by immunization with EGFR extracellular domain [20]. Using the syngeneic tumor model D122, a C57BL/6-derived metastatic clone of the Lewis lung carcinoma, 7A7 mAb showed its capacity to induce conventional mechanisms associated with EGFR inhibition [21]. 7A7 mAb inhibits not only the phosphorylation of this receptor but also the activation of several signal transduction pathways downstream EGFR, and, in consequence, several pro-tumoral processes activated through this signaling. Also, 7A7 mAb induces a specific *in vitro* ADCC on these tumor cells and a potent *in vivo* anti-metastatic effect on this model. This *in vivo* activity completely relays on CD8+ and CD4+ T cells [21]. To study the contribution of both, EGFR pharmacological blockade and Fc region to the immune response induced by 7A7 mAb, we intended to use its bivalent $F(ab')_2$ fragment. Our group previously demonstrated that this fragment has the same antitumoral activity *in vitro* compared with the whole Ab [22]. To accomplish *in vivo* experiments, a previous selection of the optimal treatment regimen requires a thorough understanding and comparison of the pharmacokinetics of 7A7 whole mAb and its $F(ab')_2$ fragment. In this study we assessed some pharmacokinetics parameters and the biodistribution after intravenous (i.v.) administration of a single dose of ^{125}I-labeled 7A7 mAb to immunocompetent C57BL/6 mice. We also measured 7A7 mAb and 7A7 $F(ab')_2$ by an ELISA technique validating this method to evaluate pharmacokinetics of this mAb.

2. Methods

2.1. Mice. Female C57BL/6 mice at 6–8 weeks of age (average weight, 20 g) were purchased from the National Center for the Laboratory Animals Production (CENPALAB, Havana, Cuba). Animals were housed under pathogen-free conditions and all procedures were approved by CIM Institutional Animal Care and Use Committee (Havana, Cuba) and the Center for Radiation Protection and Hygiene (Havana, Cuba). Animals were kept with a 12-hour light-dark cycle and *ad libitum* access to water and standard food pellets. Blood samples were collected separately from each mouse via the retro orbital sinus of the eye by ocular puncture. Anesthesia was not used during the study.

2.2. Antibody and Preparation of $F(ab')_2$ Fragment. 7A7 mAb was obtained at CIM [20]. The $F(ab')_2$ fragment of 7A7 mAb was obtained by pepsin digestion. Briefly, 7A7 mAb was brought to 2 mg/mL and dialyzed overnight versus 0.1 M acetate buffer (pH 3.8). Pepsin (Sigma-Aldrich, St. Louis, MO, USA) was added at 37°C for 4 h with agitation. Digestion was stopped increasing pH to 8.0 with a 3 M Tris-HCl buffer and was followed by extensive overnight dialysis against phosphate buffered saline (PBS) pH 7.4. Undigested mAb and small peptides were separated from 7A7 $F(ab')_2$ fragments by passing the mixture by a Sepharose SpA column from GE Healthcare Life sciences (BUCKinghamshire,UK), equilibrated with PBS. $F(ab')_2$ fragment-containing fraction was extensively dialyzed against PBS. After concentration, $F(ab')_2$ fragment was sterilized by filtration through a 0.22 μm filter (Millipore, Billerica, MA, USA) and stored in aliquots at 4°C until being used. The purity of fragment was analyzed by 10% and 7.5% SDS-PAGE under reducing and non-reducing conditions, respectively [23]. Gels were stained by Coomassie Blue with an aqueous solution containing 0.1% PhastGel Blue R (Sigma-Aldrich), 10% acetic acid, and 30% methanol and destained with a solution consisting of 10% acetic acid and 30% methanol. Protein molecular weight markers from GE Healthcare Lifesciences and from Bio-Rad Laboratories were used for a comparison. Purity of $F(ab')_2$ fraction was assessed by densitometry using a personal densitometer SI (GE Healthcare Lifesciences) and Image Quant Software.

2.3. Pharmacokinetics and Biodistribution of ^{125}I-7A7 mAb. 7A7 mAb labeling was performed at the Development Department of the Isotope Center, Havana, Cuba. 7A7 mAb was labeled with ^{125}I using the Iodo-Gen procedure [24] and labeled fractions were purified by molecular exclusion using a PD10 column Sephadex G25 (GE Healthcare Lifesciences). ^{125}I-labeled 7A7 mAb (2.8 mg per Kg/12.0 MBq/mg) was administered to mice in 0.1 mL by an i.v. bolus infusion via lateral tail vein. Following i.v. injection, blood samples were taken in each group (n = 3) at time intervals (1, 10, and 30 min and 1, 4, 8, 12, 24, and 48 h post-injection). Plasma samples were immediately mixed with 1 mL of 0.1% bovine serum albumin (BSA) solution. Trichloroacetic acid (TCA) was added to a final concentration of 10% and samples were centrifuged at 4°C for 10 min at 1000 ×g. Radioactivity in the precipitated was counted with an automatic γ-counter (Berthold LB 2104, Berthold Technologies, Bad Wildbad, Germany). After blood drawal, same groups of three mice were sacrificed and liver, kidneys, lungs, and spleen were

excised, rinsed of residual blood, and weighted. Samples were counted for radioactivity. Organ activity was expressed as the percentage of the injected dose per gram of tissue (% D/g).

2.4. Pharmacokinetics of 7A7 mAb and 7A7 F(ab′)$_2$ Fragment by ELISA. Non-labeled 7A7 mAb (2.8 mg per Kg) and non-labeled 7A7 F(ab′)$_2$ fragments (1.86 mg per Kg) were administered to mice in 0.1 mL by i.v. bolus infusion via lateral tail vein. Following i.v. injection, blood samples were taken in each group ($n = 3$) at time intervals (1, 10, and 30 min and 1, 4, 8, 12, 24, and 48 h post-injection). Whole blood was immediately taken through heparin-coating capillaries. Concentration of non-labeled 7A7 mAb and 7A7 F(ab′)$_2$ fragment in plasma samples was measured using an ELISA system. Ninety-six wells microtiter plates (High Binding, Costar, Corning Inc., NY, USA) were coated with the recombinant extracellular domain of murine EGFR (mECD) [25] at a concentration of 5 μg/mL in a carbonate buffer, 0.1 M, pH 9.6, and were incubated overnight at 4°C. After washing three times with PBS containing 0.05% Tween20, plates were blocked with 5% fetal calf serum in PBS/Tween20. Standard curves for mAb and F(ab′)$_2$ fragment ranging from 3.9 ng/mL to 500 ng/mL were added to the plates for 1 h at 37°C. Plasma samples collected at each time were first tested using several dilutions (1/100, 1/500, 1/1 000, 1/5 000, and 1/10 000) in order to obtain parallel descending curves. Dilutions of 1/1 000 for mAb containing fractions and 1/500 dilution for F(ab′)$_2$ containing fractions were selected for the final analysis. In all cases detection was achieved by the addition of biotin-goat anti-mouse Fab conjugate (Sigma-Aldrich) during 1 h at 37°C followed by an alkaline phosphatase-streptavidin conjugate (Sigma-Aldrich) in the same conditions. After the addition of *p*-nitrophenyl-phosphate (1 mg/mL) (Sigma-Aldrich) in diethanolamine buffer pH 9.8, absorbance at 405 nm was read with a Microwell System reader (Organon Teknika Inc., Salzburg, Austria).

2.5. Pharmacokinetics Data Analysis. In both cases of labeled and non-labeled plasma samples, total counts or absorbance units were converted to micrograms per milliliters (μg/mL) of mAb or F(ab′)$_2$ fragment using the standard curves. Pharmacokinetics parameters were obtained by fitting a two-compartment model to plasma activity in μg/mL against the time of blood drawing, using WinNonlin professional Software (WinNonlin, ver. 2.01, 1997, Pharsight Co., Virginia, USA). These include the following parameters: $t_{1/2}\beta$: elimination half-life; AUC: area under the curve; CL: clearance; Vss: volume of the distribution at a steady state. These PK parameters were generated using the equation describing a two-compartment open model with additional effect-site compartment, after an i.v. bolus input [26].

3. Results

3.1. Preparation and Biochemical Characterization of 7A7 F(ab′)$_2$ Fragment. Digestion of 7A7 mAb with pepsin and the purification of its F(ab′)$_2$ fragment were described in the experimental procedures. Figure 1 shows the purity of 7A7 fragment as determined by SDS-PAGE under reducing and non-reducing conditions. There was no detectable contamination in the preparation of F(ab′)$_2$ fragment after purification. Under non-reducing conditions, 7A7 mAb and F(ab′)$_2$ fragment showed their expected migration positions, ~150 kDa and ~100 kDa, respectively, and no intact IgG mAb molecules were detected. Under reducing conditions, 7A7 mAb is resolved into characteristic heavy (H) and light (L) chains, while F(ab′)$_2$ fragment display typical modified heavy chains (H′ chains) and unmodified L chains. *In vitro* biological activity of this molecule was previously proved, demonstrating analogous activity when compared with the whole mAb [22].

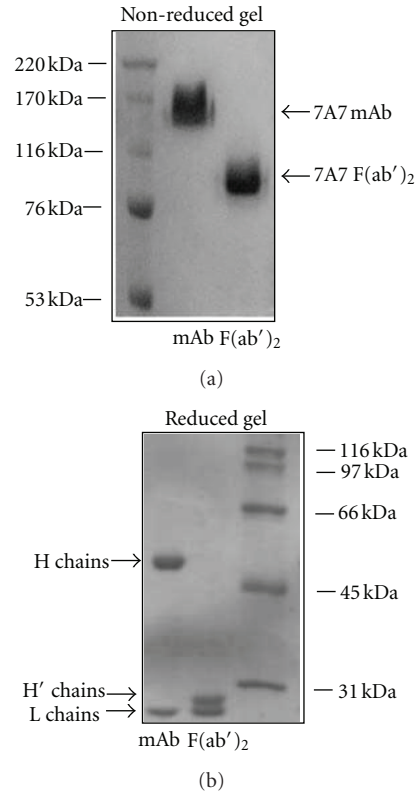

Figure 1: SDS-PAGE analysis of 7A7 mAb and 7A7 F(ab′)$_2$ fragment. 7A7 mAb and 7A7 F(ab′)$_2$ fragment were separated by SDS-PAGE under non-reducing conditions (a) and under reducing conditions with β-mercaptoethanol (b). Gels were stained with Coomassie Blue. Analysis was performed three times with similar results. Representative data are shown.

3.2. Pharmacokinetics of ^{125}I-7A7 mAb. ^{125}I-7A7 mAb was i.v. administered to mice in a single dose (2.8 mg per Kg/12.0 MBq/mg). Blood samples were taken at intervals for radioactivity determinations. Radioactivity content in mice plasma, expressed as the percentage of the injected dose per milliliter (% D/mL), was plotted against the time of blood drawing (Figure 2(a)). As observed, the radioactivity content decreases in time and the resulting plasma activity curve best fitted two-compartment analysis model as expected

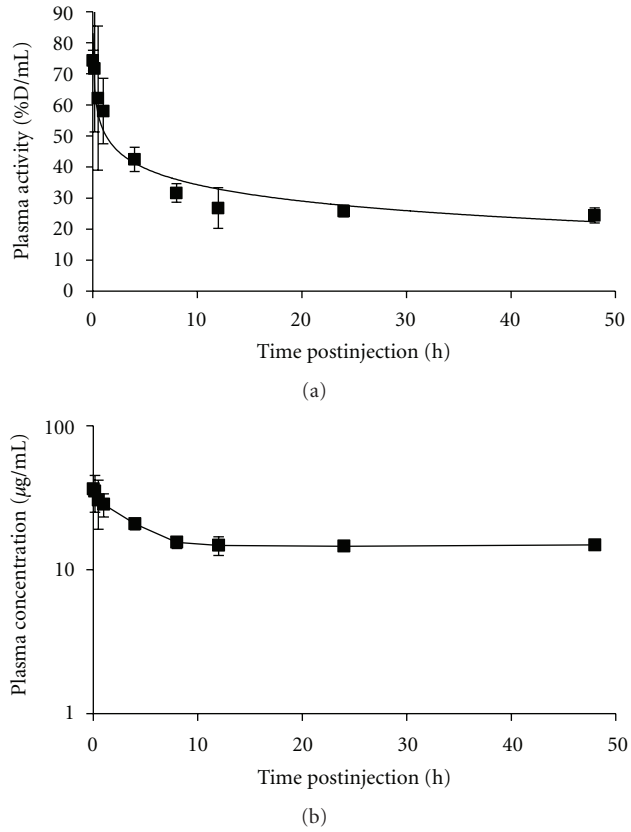

Figure 2: Plasma clearance of ^{125}I-7A7 mAb in C57BL6 mice. ^{125}I-7A7 mAb (2.8 mg per Kg/12.0 MBq/mg) was injected i.v. into C57BL6 mice. Blood samples were collected at time intervals (1, 10, and 30 min and 1, 4, 8, 12, 24, and 48 h post-injection) and immediately mixed with 1 mL of 0.1% BSA solution and TCA, and radioactivity was counted. Plasma activity measured in the percentage of dose per milliliter (% D/mL) (a) or ^{125}I-7A7 mAb plasma concentration (b) is shown. Plotted values represent mean of 3 animal's data points per group ± standard deviation (SD).

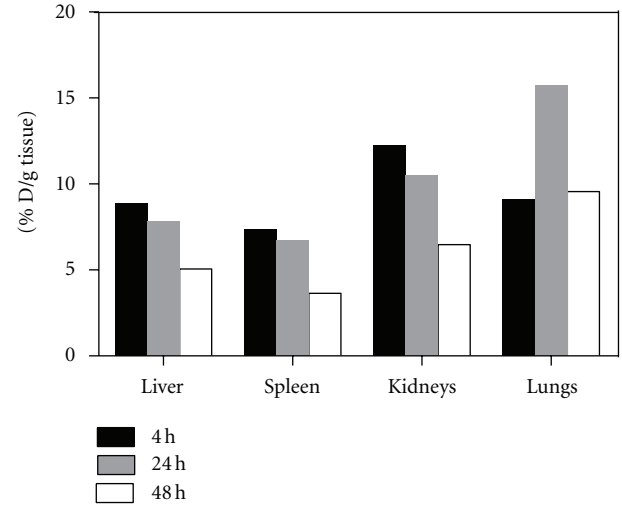

Figure 3: Biodistribution of ^{125}I-7A7 mAb in C57BL/6 mice. After a single i.v. injection of 2.8 mg per Kg of radiolabeled 7A7 mAb (12.0 MBq/mg), groups of three mice were sacrificed and liver, kidneys, lungs, and spleen were excised, rinsed of residual blood, and weighted. Radioactivity levels were measured at 4, 24, and 48 h using a γ-counter. Graphs represent the percentage of the initial injected dose/g tissue (% D/g).

for i.v. bolus injection. Plasma concentrations-time curve was obtained using % D/mL values obtained for each time point multiplied by mAb dose injected (56 μg/mouse) (Figure 2(b)). Pharmacokinetics data are shown in Table 1. 7A7 mAb displayed a $t_{1/2}\beta$ of 23.1 ± 0.4 h. AUC was 801.1 ± 8.9 μg/mL·h and a very slow CL was observed (0.06 ± 0.001 mL/h). Vss was 1.41 ± 0.03 mL for ^{125}I-7A7 mAb.

3.3. Biodistribution Study of ^{125}I-7A7 mAb. After i.v. administration of ^{125}I-7A7 mAb, groups of mice ($n = 3$) were sacrificed at 4, 24, and 48 h. Liver, lungs, kidneys, and spleen were removed and counted for radioactivity. Time courses of radioactivity in the organs showed the uptake of the labeled mAb by these organs (Figure 3) and the subsequence time-dependent elimination. 7A7 mAb showed a tendency toward decrease accumulation in time. However, a higher accumulation of the radiolabeled mAb was found in lungs 24 h after injection (15.76 ± 1.10% D/g) when comparing with the other organs (7.81±1.05% D/g for liver, 6.72±1.28% D/g for spleen, and 10.52 ± 2.27% D/g for kidneys).

3.4. Pharmacokinetics of 7A7 mAb and Its F(ab′)$_2$ Fragment. Equimolar concentrations of non-labeled 7A7 mAb (2.8 mg per Kg) and non-labeled F(ab′)$_2$ fragment (1.86 mg per Kg) were injected i.v. into mice. Plasma samples were collected after 1, 10, and 30 min and 1, 4, 8, 12, and 48 h post-injection of 7A7 mAb or 7A7 F(ab′)$_2$ fragment. Presence of both molecules was determined by the ELISA system described previously. Plasma concentrations at each time point were determined plotting absorbance values on standard curves for both molecules. Obtained plasma concentration curves also fitted a two-compartment analysis model (Figure 4). Pharmacokinetics data obtained are given in Table 2. Comparison between parameters obtained by this technique and those obtained by radioactivity validates this ELISA to study pharmacokinetics of murine anti-mouse EGFR mAbs. Using this new method, 7A7 mAb holds a $t_{1/2}\beta$ of 23.9 ± 0.7 h. This value of $t_{1/2}\beta$ was very similar to that obtained by the radioactivity method (23.1 ± 0.4 h). Additionally, clearance value for mAb (0.033 ± 0.001 mL/h) was also similar to that obtained by radioactivity (0.06 ± 0.001 mL/h). In the case of Vss, similar to values obtained by the radioactivity method (1.41 ± 0.03 mL), 7A7 mAb showed a Vss of 1.11 ± 0.01 mL by ELISA. However, major differences were obtained in the AUC. For 7A7 mAb by ELISA this value was 1680.8 ± 6.9 μg/mL·h, in contrast to 801.1 ± 8.9 μg/mL·h obtained previously. Pharmacokinetics parameters were also analyzed for 7A7 F(ab′)$_2$ fragment. This molecule displayed a ten-times lower $t_{1/2}\beta$ (2.25 ± 0.2 h) in comparison with the whole mAb. By this method F(ab′)$_2$ fragment holds a faster clearance (0.3 ± 0.007 mL/h) and a Vss of 0.94 ± 0.03 mL. AUC was 124.1 ± 5.6 μg/mL·h.

Table 1: Pharmacokinetic parameters of ^{125}I-7A7 mAb (2.8 mg per Kg/12.0 MBq/mg) after a single i.v. injection in C57BL/6 mice ($n = 3$).

	Pharmacokinetic parameters of ^{125}I-7A7 mAb in C57BL/6 mice			
	$t_{1/2}\,\beta$ (h)	AUC (μg/mL·h)	CL (mL/h)	Vss (mL)
7A7 mAb	23.1 ± 0.4	801.1 ± 8.9	0.06 ± 0.001	1.41 ± 0.03

Data are expressed as the mean ± SD.
$t_{1/2}$: elimination half-life; AUC: area under the curve; CL: clearance; Vss: volume of the distribution at a steady state.

Table 2: Pharmacokinetic parameters of 7A7 mAb (2.8 mg per Kg) or 7A7 F(ab′)$_2$ fragment (1.86 mg per Kg) after a single i.v. injection in C57BL/6 mice ($n = 3$).

	Pharmacokinetic parameters of 7A7 mAb and 7A7 F(ab′)$_2$ fragment in C57BL/6 mice			
	$t_{1/2}\beta$ (h)	AUC (μg/mL·h)	CL (mL/h)	Vss (mL)
7A7 mAb	23.9 ± 0.7	1680.8 ± 6.9	0.033 ± 0.001	1.11 ± 0.01
7A7 F(ab′)$_2$	2.25 ± 0.2	124.1 ± 5.6	0.300 ± 0.007	0.94 ± 0.03

Data are expressed as the mean ± SD.
$t_{1/2}$: eliminati on half-life; AUC: area under the curve; CL: clearance; Vss: volume of the distribution at a steady state.

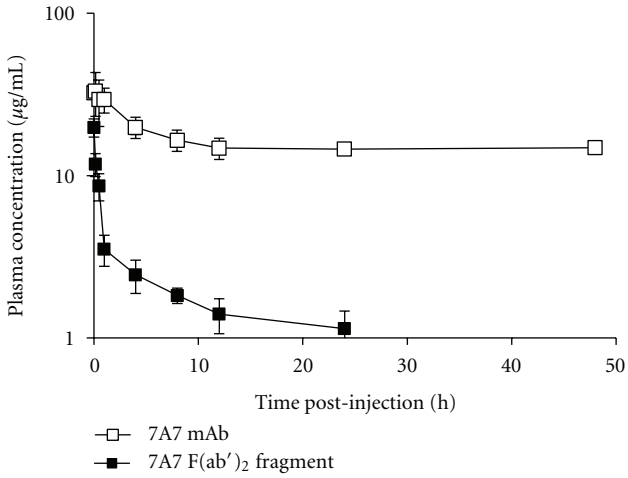

Figure 4: Plasma clearance of 7A7 mAb and 7A7 F(ab′)$_2$ fragment in C57BL6 mice. 7A7 mAb (2.8 mg per Kg) or 7A7 F(ab′)$_2$ fragment (1.86 mg per Kg) were injected i.v. into C57BL6 mice. Blood samples were collected at time intervals (1, 10, and 30 min and 1, 4, 8, 12, 24, and 48 h post-injection). Concentration of both molecules in plasma samples was measured using an ELISA system using several plasma dilutions. Absorbance units were converted to μg/mL of mAb or F(ab′)$_2$ fragment using standard curves. Plotted values represent mean of 3 animal's data points per group ± standard deviation (SD).

4. Discussion

Monoclonal antibody-based therapy constitutes one of the most suitable approaches for cancer treatment. Rituximab (anti-CD20), trastuzumab (anti-human epidermal growth factor receptor-2, HER2), cetuximab, and panitumumab are among the most successful therapeutic mAbs directed against tumor antigens. Despite an obvious clinical benefit obtained with these mAbs, a significant variability among patients' responses is observed in the clinical setting [27]. Special emphasis has received the assertion that a best therapeutic success of these agents could rely mostly on the complete elucidation of mechanisms underlying the antitumor response induced. Despite their direct effects on cell signaling pathways, the capacity of tumor antigens-specific mAbs to activate a T-cell response is not excluded as a potential mechanism of the antitumor activity. In fact, the kinetics of the clinical response observed in mAb-treated patients results in tumor shrinkage over weeks, consistent with a T-cell-mediated effect [27]. Therefore, a remarkable interest is being focused on the question if the antitumor effects are mediated by Fc-induced adaptive immunity and/or target pharmacological blockade might also contribute. To address this topic, the evaluation of the ability of these agents to activate an immune response must be incorporated into accurate models reflecting the immunologic mechanism of action, with special emphasis on T cells [19]. Several strategies have being explored to assess these issues as *Fcer1g*$^{-/-}$ mice and F(ab′)$_2$ bivalent fragments. Studies to verify the mAb-induced vaccinal effect in the preclinical scenario using F(ab′)$_2$ fragments have been conducted recently for rituximab [28] and trastuzumab [29]. Experiments conducted with the F(ab′)$_2$ fragment of 225 mAb (the mouse counterpart of cetuximab) demonstrated that *in vivo* antitumor effect can be achieved with the pharmacological blockade of EGFR. Nevertheless, their findings also suggested that immune mechanisms may be contributing to the antitumor activity induced by the whole Ab [30]. However, since mAbs targeting EGFR does not cross-react with the murine molecule this research was carried out on xenografted nude mice. Therefore, the involvement of T cells in the effect of these agents had not been investigated so far. This confirms the idea of using immunocompetent mice as the most important strategies to explore this issue.

The rationale to assess the contribution of immune mechanisms to the antitumor effects of anti-EGFR mAbs in immunocompetent mice was confronted by our group by the previous generation of a mAb that recognizes murine EGFR, named 7A7 [20]. This mAb induces a potent anti-metastatic effect on D122 tumor model when given in prophylactic or therapeutic schedules [21]. This same study showed that T-CD4+ and T-CD8+ cell responses were required for the 7A7 mAb anti-metastatic effect on

D122 tumor. Because of the differences in the molecular weights of the $F(ab')_2$ fragment and their corresponding IgG, and the described differences in clearance by the reticuloendothelial system and excretion by the kidneys [31], the performance of a pharmacokinetics study before *in vivo* comparisons of the effects of both molecules, regardless of the biological model used, is generally accepted. To carry out the pharmacokinetics of 7A7 mAb, in this report we selected a single i.v. infusion of 2.8 mg per Kg according to previous studies [21, 22]. Equimolar concentrations of whole Ab and bivalent fragment were individually administered. Elimination half-life of ^{125}I-labeled 7A7 mAb after a single i.v. injection was 23.1 h. We selected this radioactivity method as the most suitable approach to evaluate mAb pharmacokinetics on preclinical models [30, 32]. However, given the advantage of possessing an autologous model, we adapted a previously described ELISA system using mECD [25] to directly evaluate the presence of 7A7 mAb in blood samples. This allows us to circumvent the main drawbacks of the use of radioactivity methods. Pharmacokinetics analyses using similar approaches involving an ELISA system with blood fractions and specific ligands have been reported and validated by other authors [33–35]. This analysis gave a $t_{1/2}\beta$ for 7A7 mAb of 23.9 h, very similar to the value of $t_{1/2}\beta$ obtained using the radioactivity method. For the $F(ab')_2$ fragment, a ten-fold lower half-time was found. In addition, 7A7 $F(ab')_2$ fragment clearance occurred in a faster manner than mAb's in agreement with $t_{1/2}\beta$ results. Noteworthy, the obtained half-time for 7A7 mAb in both experimental approaches is an "apparent" half-life over the first 48 h of the elimination curve. Given the fact that this curve ends as a plateau, the final elimination could take place with its intrinsic half-life. Further experiments should be accomplished in order to complete this measurement.

Our data support the use of the 7A7 $F(ab')_2$ fragment in *in vivo* studies to explore the contribution of EGFR signaling inhibition and Fc portion to the CTL response induced by 7A7 mAb. The short half-life obtained for 7A7 $F(ab')_2$ suggests that extremely large amounts of the fragment would have to be continuously infused, in order to obtain plasma concentrations which could account for the same concentration of the whole Ab injected. However, our experimental setting and the 10-fold difference in half-life values does not allow us to follow this approach. Instead, we used another strategy previously described [32], in which the dose used for *in vivo* therapy was adjusted based on the $t_{1/2}\beta$ observed for anti-HER2 mAb and their bivalent fragments. Since a difference in a 5-fold higher value was found in this study, 5-fold larger amounts of the $F(ab')_2$ fragments were administered [32]. In our subsequent research, we used therefore this experimental procedure injecting equimolar concentrations of both molecules, 7A7 mAb and its $F(ab')_2$ fragment. Our results demonstrated that EGFR pharmacological blockade by both molecules contributes to the antimetastatic effect induced by 7A7 mAb and is able to connect with adaptive immune system activation [22].

In the present report we conducted biodistribution studies to investigate 7A7 mAb localization after injection. The uptake in the most important source organs, lungs, liver, kidneys, and spleen was determined as a function of time. We found a significant higher accumulation of mAb in lungs even 48 h after the injection. This observation gets a significant value and supports the syngeneic tumor cell model used previously by our group, the experimental metastasis model of C57BL/6 derived D122 metastatic clone of the Lewis lung carcinoma [36]. Our group demonstrated the potent anti-metastatic effect of 7A7 mAb on this cell model [21]. Further studies showed that a single dose of 7A7 mAb given at day 6 after tumor inoculation induces an anti-metastatic effect identical to that produced by 6 doses of Ab [22]. This seems to be in agreement with the results of biodistribution in which 7A7 appears to hold a particular preference for lungs even in the absence of the tumor, thus facilitating its access to this organ. Kidneys also possess a high accumulation of 7A7 mAb after 48 h. This might suggest a radiopharmaceutical clearance via the urinary bladder route [37].

Murine mAbs are extremely valuable tools to perform studies in animal models that may help to improve human mAb-based immunotherapy. Even when the behavior of mAbs may differ notably interspecies, similarities in pharmacokinetics can be found. For example, a study conducted at CIM and carried out in patients using nimotuzumab showed that one single dose by i.v. injection produces an accumulation of this mAb in liver, heart, urinary bladder, and spleen, preferentially, with longer persistency in kidneys [38]. Therefore, nimotuzumab seems to share common excretion pathways with 7A7 mAb. In addition, plasma disappearance curves of nimotuzumab were best fit by a biexponential equation. This study showed great similarities in the pharmacokinetics of murine and human mAbs targeting EGFR. This seems to overcome the possible species differences in the antibody-antigen binding and the impact of antigen binding on Ab kinetics. However, possible differences in binding to the FcRn receptor between species and the immunogenic potential of the mAb interspecies should also be considered.

5. Conclusions

Using the valuable results obtained in this report with 7A7 mAb and its $F(ab')_2$ fragment, we demonstrated that EGFR signaling blockade is able to induce a specific CTL response [22]. However, the Fc region contribution and even the isotype relevance for this response might be assessed. Further evaluations could subsequently be done with other biological tools such as $Fcer1g^{-/-}$ mice and/or molecular engineered Abs to reduce or lose affinity for FcγRIII on immune effector cells.

Conflict of Interests

The authors have no financial conflicts of interest.

References

[1] J. M. Reichert and E. Dhimolea, "The future of antibodies as cancer drugs," *Drug Discovery Today*, vol. 17, no. 17-18, pp. 954–963, 2012.

[2] T. Crombet, M. Osorio, T. Cruz et al., "Use of the humanized anti-epidermal growth factor receptor monoclonal antibody h-R3 in combination with radiotherapy in the treatment of locally advanced head and neck cancer patients," *Journal of Clinical Oncology*, vol. 22, no. 9, pp. 1646–1654, 2004.

[3] M. O. Rodríguez, T. C. Rivero, R. D. C. Bahi et al., "Nimotuzumab plus radiotherapy for unresectable squamous-cell carcinoma of the head and neck," *Cancer Biology and Therapy*, vol. 9, no. 5, pp. 343–349, 2010.

[4] T. C. Ramos, J. Figueredo, M. Catala et al., "Treatment of high-grade glioma patients with the humanized anti-epidermal growth factor receptor (EGFR) antibody h-R3: report from a phase I/II trial," *Cancer Biology and Therapy*, vol. 5, no. 4, pp. 375–379, 2006.

[5] G. Saurez, R. Cabanas, M. Zaldivar et al., "Clinical experience with nimotuzumab in Cuban pediatric patients with brain tumors, 2005 to 2007," *MEDICC Review*, vol. 11, no. 3, pp. 27–33, 2009.

[6] M. Ramos-Suzarte, P. Lorenzo-Luaces, N. G. Lazo et al., "Treatment of malignant, non-resectable, epithelial origin esophageal tumours with the humanized anti-epidermal growth factor antibody nimotuzumab combined with radiation therapy and chemotherapy," *Cancer Biology & Therapy*, vol. 13, no. 8, pp. 600–605, 2012.

[7] G. Bebb, C. Smith, S. Rorke et al., "Phase i clinical trial of the anti-EGFR monoclonal antibody nimotuzumab with concurrent external thoracic radiotherapy in Canadian patients diagnosed with stage IIb, III or IV non-small cell lung cancer unsuitable for radical therapy," *Cancer Chemotherapy and Pharmacology*, vol. 67, no. 4, pp. 837–845, 2011.

[8] M. Massimino, U. Bode, V. Biassoni, and G. Fleischhack, "Nimotuzumab for pediatric diffuse intrinsic pontine gliomas," *Expert Opinion on Biological Therapy*, vol. 11, no. 2, pp. 247–256, 2011.

[9] D. Strumberg, B. Schultheis, M. E. Scheulen et al., "Phase II study of nimotuzumab, a humanized monoclonal anti-epidermal growth factor receptor (EGFR) antibody, in patients with locally advanced or metastatic pancreatic cancer," *Investigational New Drugs*, pp. 1–6, 2010.

[10] R. Perez, E. Moreno, G. Garrido, and T. Crombet, "EGFR-targeting as a biological therapy: understanding Nimotuzumab's clinical effects," *Cancers*, vol. 3, no. 2, pp. 2014–2031, 2011.

[11] M. Peipp, M. Dechant, and T. Valerius, "Effector mechanisms of therapeutic antibodies against ErbB receptors," *Current Opinion in Immunology*, vol. 20, no. 4, pp. 436–443, 2008.

[12] E. Martinelli, R. De Palma, M. Orditura, F. De Vita, and F. Ciardiello, "Anti-epidermal growth factor receptor monoclonal antibodies in cancer therapy," *Clinical and Experimental Immunology*, vol. 158, no. 1, pp. 1–9, 2009.

[13] A. López-Albaitero and R. L. Ferris, "Immune activation by epidermal growth factor receptor-specific monoclonal antibody therapy for head and neck cancer," *Archives of Otolaryngology*, vol. 133, no. 12, pp. 1277–1281, 2007.

[14] W. Zhang, M. Gordon, A. M. Schultheis et al., "FCGR2A and FCGR3A polymorphisms associated with clinical outcome of epidermal growth factor receptor-expressing metastatic colorectal cancer patients treated with single-agent cetuximab," *Journal of Clinical Oncology*, vol. 25, no. 24, pp. 3712–3718, 2007.

[15] A. López-Albaitero, S. C. Lee, S. Morgan et al., "Role of polymorphic Fc gamma receptor IIIa and EGFR expression level in cetuximab mediated, NK cell dependent *in vitro* cytotoxicity of head and neck squamous cell carcinoma cells," *Cancer Immunology*, vol. 58, no. 11, pp. 1855–1864, 2009.

[16] T. Schneider-Merck, J. J. Van Lammerts Bueren, S. Berger et al., "Human IgG2 antibodies against epidermal growth factor receptor effectively trigger antibody-dependent cellular cytotoxicity but, in contrast to IgG1, only by cells of myeloid lineage," *Journal of Immunology*, vol. 184, no. 1, pp. 512–520, 2010.

[17] J. A. Bonner, P. M. Harari, J. Giralt et al., "Radiotherapy plus cetuximab for squamous-cell carcinoma of the head and neck," *New England Journal of Medicine*, vol. 354, no. 6, pp. 567–578, 2006.

[18] P. V. Beum, D. A. Mack, A. W. Pawluczkowycz, M. A. Lindorfer, and R. P. Taylor, "Binding of rituximab, trastuzumab, cetuximab, or mAb T101 to cancer cells promotes trogocytosis mediated by THP-1 cells and monocytes," *Journal of Immunology*, vol. 181, no. 11, pp. 8120–8132, 2009.

[19] S. C. Lee, R. M. Srivastava, A. López-Albaitero, S. Ferrone, and R. L. Ferris, "Natural killer (NK):dendritic cell (DC) cross talk induced by therapeutic monoclonal antibody triggers tumor antigen-specific T cell immunity," *Immunologic Research*, vol. 50, no. 2-3, pp. 248–254, 2011.

[20] G. Garrido, B. Sanchez, H. M. Rodriguez, P. Lorenzano, D. Alonso, and L. E. Fernandez, "7A7 MAb: a new tool for the pre-clinical evaluation of EGFR-based therapies," *Hybridoma and Hybridomics*, vol. 23, no. 3, pp. 168–175, 2004.

[21] G. Garrido, P. Lorenzano, B. Sánchez et al., "T cells are crucial for the anti-metastatic effect of anti-epidermal growth factor receptor antibodies," *Cancer Immunology*, vol. 56, no. 11, pp. 1701–1710, 2007.

[22] G. Garrido, A. Rabasa, B. Sanchez et al., "Induction of immunogenic apoptosis by blockade of epidermal growth factor receptor activation with a specific antibody," *Journal of Immunology*, vol. 187, no. 10, pp. 4954–4966, 2011.

[23] U. K. Laemmli, "Cleavage of structural proteins during the assembly of the head of bacteriophage T4," *Nature*, vol. 227, no. 5259, pp. 680–685, 1970.

[24] P. J. Fraker and J. C. Speck Jr, "Protein and cell membrane iodinations with a sparingly soluble chloroamide, 1,3,4,6-tetrachloro-3a,6a-diphenylglycoluril," *Biochemical and Biophysical Research Communications*, vol. 80, no. 4, pp. 849–857, 1978.

[25] B. S. Ramírez, E. S. Pestana, G. G. Hidalgo et al., "Active antimetastatic immunotherapy in Lewis lung carcinoma with self EGFR extracellular domain protein in VSSP adjuvant," *International Journal of Cancer*, vol. 119, no. 9, pp. 2190–2199, 2006.

[26] N. H. G. Holford and L. B. Sheiner, "Understanding the dose-effect relationship: clinical application of pharmacokinetic-pharmacodynamic models," *Clinical Pharmacokinetics*, vol. 6, no. 6, pp. 429–453, 1981.

[27] R. L. Ferris, E. M. Jaffee, and S. Ferrone, "Tumor antigen-targeted, monoclonal antibody-based immunotherapy: clinical response, cellular immunity, and immunoescape," *Journal of Clinical Oncology*, vol. 28, no. 28, pp. 4390–4399, 2010.

[28] R. Abès, E. Gélizé, W. H. Fridman, and J. L. Teillaud, "Long-lasting antitumor protection by anti-CD20 antibody through cellular immune response," *Blood*, vol. 116, no. 6, pp. 926–934, 2010.

[29] S. Park, Z. Jiang, E. D. Mortenson et al., "The therapeutic effect of anti-HER2/neu antibody depends on both innate and adaptive immunity," *Cancer Cell*, vol. 18, no. 2, pp. 160–170, 2010.

[30] Z. Fan, H. Masui, I. Altas, and J. Mendelsohn, "Blockade of epidermal growth factor receptor function by bivalent and monovalent fragments of 225 anti-epidermal growth factor receptor monoclonal antibodies," *Cancer Research*, vol. 53, no. 18, pp. 4322–4328, 1993.

[31] D. G. Covell, J. Barbet, and O. D. Holton, "Pharmacokinetics of monoclonal immunoglobulin G1, $F(ab')_2$, and Fab' in mice," *Cancer Research*, vol. 46, no. 8, pp. 3969–3978, 1986.

[32] C. I. Spiridon, S. Guinn, and E. S. Vitetta, "A comparison of the M*in vitro* and *in vivo* activities of IgG and $F(ab')_2$ fragments of a mixture of three monoclonal anti-Her-2 antibodies," *Clinical Cancer Research*, vol. 10, no. 10, pp. 3542–3551, 2004.

[33] X. Rong, Y. Y. Xiao, F. Y. Dao, Y. Z. Chang, L. G. Pei, and D. Z. Fan, "Phase I evaluation of the safety and pharmacokinetics of a single-dose intravenous injection of a murine monoclonal antibody against hantaan virus in healthy volunteers," *Antimicrobial Agents and Chemotherapy*, vol. 53, no. 12, pp. 5055–5059, 2009.

[34] T. Puchalski, U. Prabhakar, Q. Jiao, B. Berns, and H. M. Davis, "Pharmacokinetic and pharmacodynamic modeling of an anti-interleukin-6 chimeric monoclonal antibody (siltuximab) in patients with metastatic renal cell carcinoma," *Clinical Cancer Research*, vol. 16, no. 5, pp. 1652–1661, 2010.

[35] T. Miyake, O. Sawada, M. Kakinoki et al., "Pharmacokinetics of bevacizumab and its effect on vascular endothelial growth factor after intravitreal injection of bevacizumab in macaque eyes," *Investigative Ophthalmology and Visual Science*, vol. 51, no. 3, pp. 1606–1608, 2010.

[36] L. Eisenbach, N. Hollander, and L. Greenfeld, "The differential expression of H-2K versus H-2D antigens, distinguishing high- metastatic from low- metastatic clones, is correlated with the immunogenic properties of the tumor cells," *International Journal of Cancer*, vol. 34, no. 4, pp. 567–573, 1984.

[37] N. Iznaga Escobar, A. Morales Morales, J. Ducongé, I. Caballero Torres, E. Fernández, and J. A. Gómez, "Pharmacokinetics, biodistribution and dosimetry of 99mTc labeled anti-human epidermal growth factor receptor humanized monoclonal antibody R3 in rats," *Nuclear Medicine and Biology*, vol. 25, no. 1, pp. 17–23, 1998.

[38] T. Crombet, L. Torres, E. Neninger et al., "Pharmacological evaluation of humanized anti-epidermal growth factor receptor, monoclonal antibody h-R3, in patients with advanced epithelial-derived cancer," *Journal of Immunotherapy*, vol. 26, no. 2, pp. 139–148, 2003.